Stem Cell Reports, Volume *9*

Supplemental Information

Targeted Disruption of *TCF12* Reveals HEB as Essential in Human Mesodermal Specification and Hematopoiesis

Yang Li, Patrick M. Brauer, Jastaranpreet Singh, Sintia Xhiku, Kogulan Yoganathan, Juan Carlos Zúñiga-Pflücker, and Michele K. Anderson

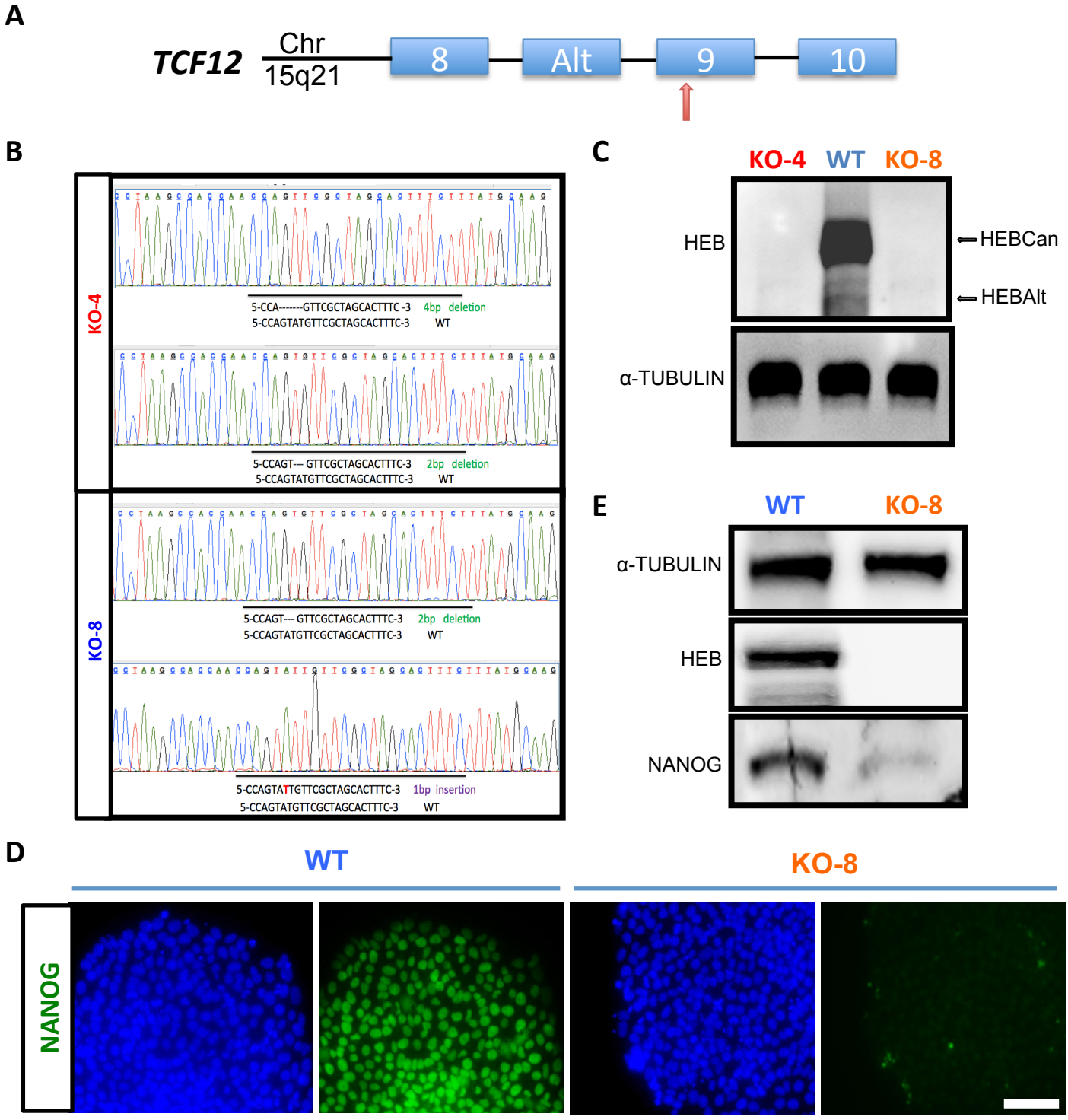

Figure S1. Generation of HEB$^{-/-}$ hESC lines KO-4 and KO-8 by CRISPR-Cas9 targeting of the *TCF12* gene locus. Related to Figure 1. (A) Schematic of the Cas9/gRNA-target site in exon 9 of the *TCF12* locus. (B) Sanger sequencing of genomic DNA from two HEB$^{-/-}$ clones (KO-4 and KO-8) comparing the sequences to WT. Each clone has two independently disrupted *TCF12* alleles. (C) Western blot analysis for HEB protein expression in WT and HEB$^{-/-}$ ESCs for both KO-4 and KO-8 (D, E) Immunofluorescent staining (D) and Western blot (E) analysis for NANOG expression in WT and KO-8 hESCs. α-TUBULIN was analyzed as a loading control. Scale bar, 100 μm. Images in C, D, and E are representative of 3 independent experiments.

A

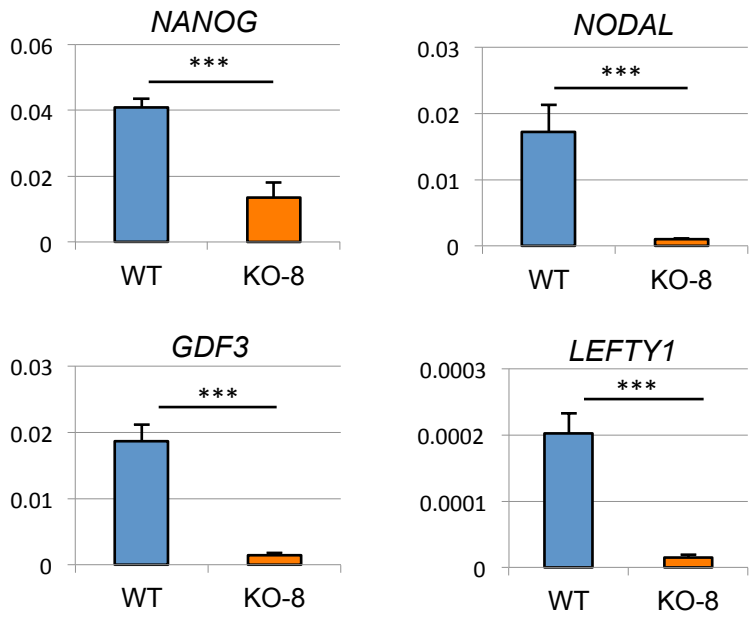

B

Gene Ontology Term	Count	P Value
GO:0007507~heart development	20	1.06E-09
GO:0044421~extracellular region part	38	6.30E-08
GO:0005576~extracellular region	59	1.94E-07
GO:0042127~regulation of cell proliferation	33	5.66E-07
GO:0007389~pattern specification process	18	9.68E-07
GO:0014032~neural crest cell development	7	1.04E-05
GO:0014033~neural crest cell differentiation	7	1.04E-05
GO:0048762~mesenchymal cell differentiation	8	1.31E-05
GO:0014031~mesenchymal cell development	8	1.31E-05
GO:0060485~mesenchyme development	8	1.50E-05
GO:0005578~proteinaceous extracellular matrix	17	2.30E-05
GO:0040008~regulation of growth	18	2.52E-05
GO:0048598~embryonic morphogenesis	17	2.56E-05
GO:0005615~extracellular space	26	2.86E-05
GO:0001944~vasculature development	15	4.01E-05

Figure S2. **Gene expression differences between WT and HEB$^{-/-}$ hESCs.** Related to Figure 2. (A) qRT-PCR analysis of the mRNA expression of pluripotency-associated genes in WT and KO-8 hESCs, normalized to *GAPDH*. (B) Gene Ontology (GO) terms for genes showing a >2-fold change between WT versus HEB$^{-/-}$ hESCs (KO-4) by RNA-seq analysis. Error bars represent mean ± SD (n=3 independent experiments). Student's *t*-test: **p<0.01; ***p<0.005.

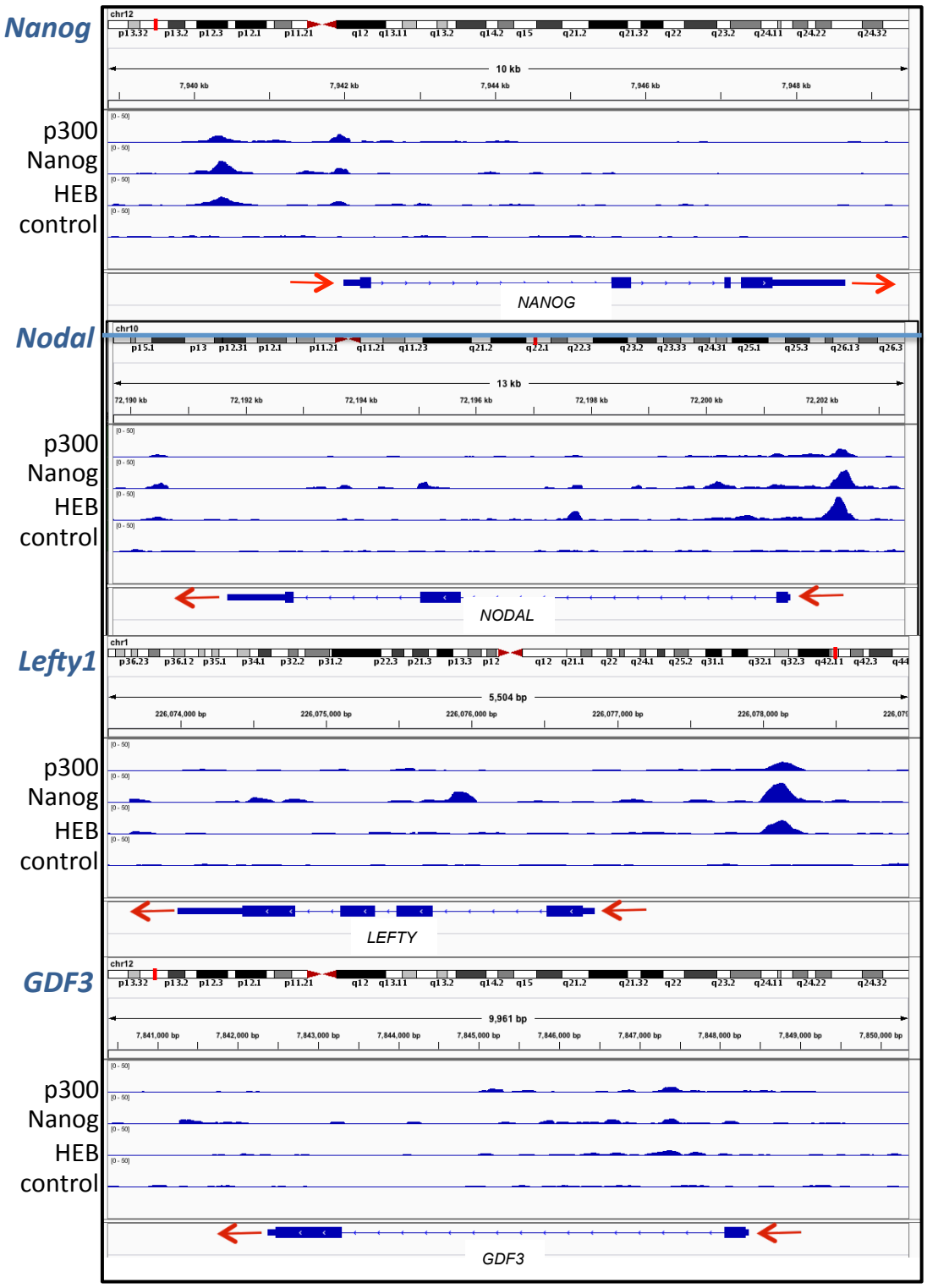

Figure S3. Direct binding of HEB to gene loci that are involved in ESC and mesoendodermal differentiation as revealed by ChIP-seq analysis. Related to Figure 2. The Integrative Genome Viewer (IGV) was used to search for peaks in H1-hESCs that corresponded to binding of HEB (TCF12), NANOG, and p300 using ChIP-seq data from the Encyclopedia of DNA Elements (ENCODE) project. The transcriptional orientation of each locus is depicted by red arrows. The names of the gene loci (blue) and the anti-transcription factor antibodies used to detect binding (black) are indicated to the left of the tracks. The intron-exon boundaries are depicted below the tracks and chromosomal locations are depicted above the tracks. The scale for all tracks is 0-50. The GEO accession numbers for these tracks are GSM803437 (NANOG), GSM803427 (TCF12), GSM803542 (p300), and GSM1010818 (control).

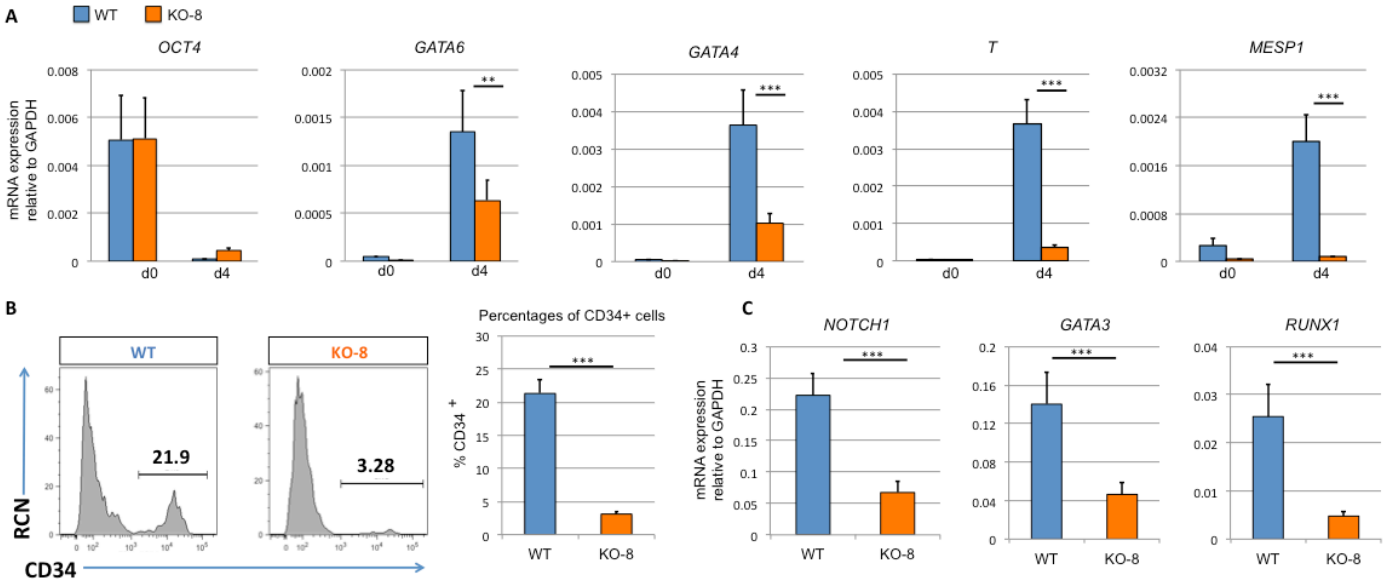

Figure S4. Experimental results comparing WT to the KO-8 HEB$^{-/-}$ hESC line. Related to Figure 3. (A) qRT-PCR analysis for the expression of pluripotency and differentiation markers in undifferentiated hESCs (d0) and day 4 (d4) EBs. mRNA levels are shown relative to GAPDH. (B) Flow cytometric analysis for percentages of CD34^{+} cells in WT and KO-8 d8 EBs. (C) qRT-PCR analysis for the expression of hematopoietic genes in CD34^{+} cells. For all qRT-PCR experiments, mRNA levels are shown relative to GAPDH. Error bars represent mean ± SD (n=3 independent experiments). Student's *t*-test: **p<0.01; ***p<0.005. Plots in B are representative of 3 independent experiments.

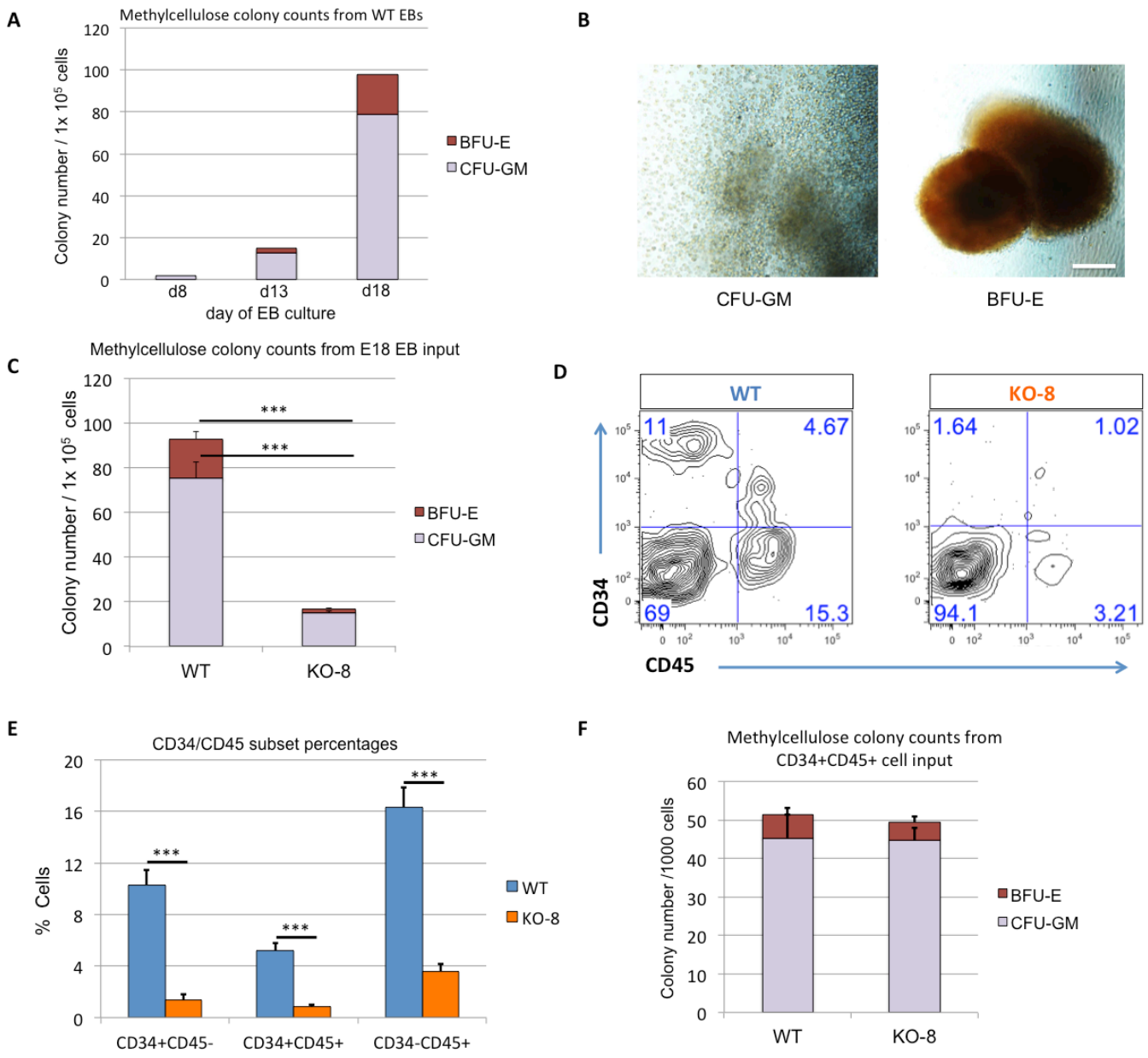

Figure S5. Myeloerythroid assays of cells derived from WT or KO-8 d18 EBs. Related to Figure 5. (A) Erythroid (BFU-E) and myeloid (CFU-GM) colony counts of cells arising from precursors obtained from WT d8, d13, and d18 EB cultures. (B) Representative images of hematopoietic colonies. (C) Erythroid (BFU-E) and myeloid (CFU-GM) colony counts of cells arising from WT and KO-8 d18 EBs. (D) Flow cytometric analysis for CD34 and CD45 expression of WT and KO-8 d18 EB-derived cells. (E) Percentage of each CD34/CD45 fraction within WT and KO-8 d18 EB-derived cells. (F) Erythroid (BFU-E) and myeloid (CFU-GM) colony counts arising from the $CD34^+$ $CD45^+$ fractions of WT and KO-8 d18 EBs. Error bars represent mean ± SD (n=3 independent experiments). Student's *t*-test: ***p<0.005. Plots in D are representative of 3 independent experiments.

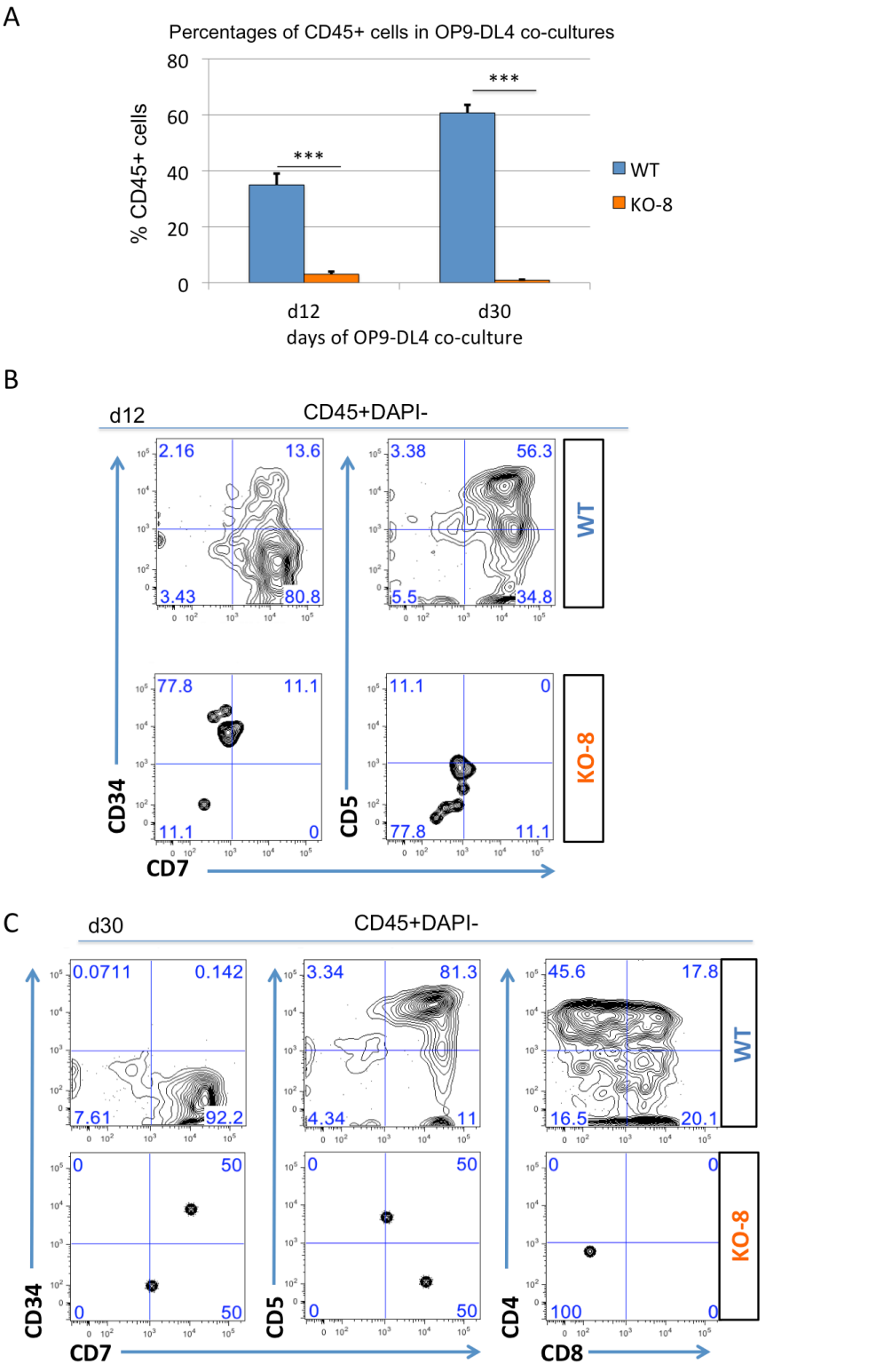

Figure S6. Assessment of hematopoietic potential of WT versus KO-8 CD34⁺ d8 EB-derived precursors on OP9-DL4 cells. Related to Figure 5. (A) Percentage of CD45⁺ cells in OP9-DL4 cells cultured with WT or KO-8 CD34⁺ cells at day 12 and day 30, as assessed by flow cytometry. (B, C) Flow cytometric analysis of T-cell development for the indicated cell surface markers from WT and KO-8 OP9-DL4 co-cultures at day 12 (B) and day 30 (C). Plots depicting T-cell markers are gated on the CD45⁺ DAPI⁻ population. Error bars represent mean ± SD (n=3 independent experiments). Student's *t*-test: **p<0.01; ***p<0.005. Plots in A, B, and C are representative of 3 independent experiments.

Table S1. List of primer sequences used for RT-PCR analysis. Linked to Figure 2, 3, 5, and 7.

Gene	Forward	Reverse
GAPDH	TCTCCTCTGACTTCAACAGCGAC	CCCTGTTGCTGTAGCCAAATTC
HEBCan	GGCTCATTTTCCCTGTACAGC	GAGGTCCCCAGAATTCCACC
HEBAlt	TGTGCTTATCCTGTCCCTGG	GCCTTTCCAAGTGCATCACC
VE-CADHERIN	TCACGGATAATCACGATAACAC	CCCATTGTCTGAGATGACCA
MYOCARDIN	AAATGACAGAAATGACTCAGCC	AGGATTTGGACTTTACAGCAG
TIE2	GGTGCTACTTAACAACTTACATCC	GGAGGAAGAATGTCACTAAGG
RUNX1	AGTCAGATGCAGGATACAAGG	CAATGGATCCCAGGTATTGGT
T	TATGAGCCTCGAATCCACATAGT	CCTCGTTCTGATAAGCAGTCAC
MESP1	TCGAAGTGGTTCCTTGG	TGCTTGCCTCAAAGTGTC
EOMES	GTGCCCACGTCTACCTGTG	CCTGCCCTGTTTCGTAATGAT
GATA4	GTGTCCCAGACGTTCTCAGTC	GGGAGACGCATAGCCTTGT
GATA6	CTGCGGGCTCTACAGCAAG	GTTGGCACAGGACAATCCAAG
NEUROD1	ATGACCAAATCGTACAGCGAG	GTTCATGGCTTCGAGGTCGT
CGB7	GGTGTGCAACTACCGCGAT	GGAGTCGGGATGGACTTGGA
OCT4	CTTGAATCCCGAATGGAAAGGG	GTGTATATCCCAGGGTGATCCTC
NANOG	ACAACTGGCCGAAGAATAGCA	GGTTCCCAGTCGGGTTCAC
GDF3	ACCCCAGAAGTTCCAACCTG	AGAAAGCGAAGTACATTCCCG
NODAL	CAGTACAACGCCTATCGCTGT	TGCATGGTTGGTCGGATGAAA
LEFTY1	TTGGGGACTATGGAGCTCAG	TCAAGTCCCTCGATGGCTAC
NOTCH1	CGGGTCCACCAGTTTGAATG	GTTGTATTGGTTCGGCACCAT
NOTCH2	TTTGGCAACTAACGTAGAAACTCA	TGCCAAGAGCATGAATACAGAGA
NOTCH3	ATGCAGGATAGCAAGGAGGA	AAGTGGTCCAACAGCAGCTT
NOTCH4	CCCAGGAATCTGAGATGGAA	CCACAGCAAACTGCTGACAT
GATA3	GATGGCACGGGACACTACCT	GCTCTCCTGGCTGCAGACA